Electrochemical Charging, Countercation Accommodation, and Spectrochemical Identity of Microcrystalline Solid Cobalt Hexacyanoferrate

ARTICLE *in* THE JOURNAL OF PHYSICAL CHEMISTRY B · FEBRUARY 1998

Impact Factor: 3.3 · DOI: 10.1021/jp9726495

Article

Electrochemical Charging, Countercation Accommodation, and Spectrochemical Identity of Microcrystalline Solid Cobalt Hexacyanoferrate

Pawel J. Kulesza, Marcin A. Malik, Mario Berrettoni, Marco Giorgetti, Silvia Zamponi, Roman Schmidt, and Roberto Marassi

J. Phys. Chem. B, **1998**, 102 (11), 1870-1876 • DOI: 10.1021/jp9726495

Electrochemical Charging, Countercation Accommodation, and Spectrochemical Identity of Microcrystalline Solid Cobalt Hexacyanoferrate

Pawel J. Kulesza,*,† Marcin A. Malik,†,§ Mario Berrettoni,‡ Marco Giorgetti,‡ Silvia Zamponi,‡ Roman Schmidt,† and Roberto Marassi*,‡

Department of Chemistry, University of Warsaw, Pasteura 1, PL-02-093 Warsaw, Poland, and Dipartimento di Scienze Chimiche, Universita di Camerino, via S. Agostino 1, I-62032 Camerino, Italy

Received: August 13, 1997; In Final Form: January 7, 1998

Oxidized and reduced cobalt(II) hexacyanoferrates were fabricated and characterized in the presence of alkali metal (Li^+, Na^+, K^+, Cs^+) and Co^{2+} countercations. Formal potentials of hexacyanoferrate(III,II) redox reactions are sensitive to the choice of electrolyte cation, and they correlate well with the sizes of hydrated Li^+, Na^+, and K^+. Electrochemical quartz crystal microbalance measurements clearly indicate that countercations, presumably in partially dehydrated form, are incorporated into reduced cobalt(II) hexacyanoferrate(II). The color of the system reflects primarily the oxidation state of iron sites. But the color of the reduced form is also affected by the nature of an intercalated hydrated countercation. This observation is correlated with the reversible continuous thermochromism of $K_2Co^{II}[Fe^{II}(CN)_6]*nH_2O$ that shall be attributed to the release of structural water molecules interacting with Co^{II} during heating in the temperature range 25−85 °C. It is apparent from X-ray absorption near-edge structure (XANES) experiments that the chemical environment of cobalt(II) sites is influenced by the presence of hydrated alkali metal countercations. The results are consistent with the accommodation of countercations in the lattice cavities at interstitial positions. The structural environment of iron ions was the same in all systems studied except that a chemical shift was observed due to change of the oxidation state of iron.

Introduction

Prussian Blue (PB) and related metal hexacyanoferrates[1−3] belong to the class of polymeric inorganic compounds that have been studied extensively for many years. Interesting properties, which have led to the continuous interest in these systems, include ion-exchange properties,[4,5] electrochromism,[3,6,7] mixed-valence electrical conductivity,[2,8,9] charge (electron, countercation) storage capabilities, and related ionic conductivity through zeolitic type pores.[3,8,10−13] Recently, metal hexacyanoferrates have been demonstrated to behave like molecular magnets that exhibit long-range magnetic ordering or bistability with hysteresis.[14−16]

There are uncertainties about the composition and structure of metal hexacyanoferrate films on electrodes, and there are still controversies about the mechanism of countercation displacement, accommodation, and lattice reconstruction during redox reactions in electrolytes containing various alkali metal cations. Depending on the degree peptization, PB has been described in two formulations: the so-called "soluble" form, $KFe^{III}[Fe^{II}(CN)_6]$, and the so-called "insoluble" form, $Fe^{III}_4[Fe^{II}(CN)_6]_3$.[1,17−21] In the case of related metal hexacyanoferrates, i.e., Fe^{III}-substituted analogues of PB, both "normal" (K^+-free) and countercation containing structures have also been proposed.[1,21] Electroanalytical and microgravimetric studies[8,10,11,22] of thin films of the systems show that flux of countercations provides charge balance during redox processes, thus allowing for a rapid reaction rate and minimal structure disruption.

For the "soluble" PB form, the ideal face-centered-cubic structure has been postulated[19] where the Fe^{II} (low-spin) and Fe^{III} (high-spin) ionic sites are octahedrally coordinated by −CN and −NC groups, respectively, to yield a three-dimensional network of repeating $-NC-Fe^{II}-CN-Fe^{III}-$ units. It is believed that the countercation (K^+) is located in a cavity at an interstitial site. The structure of crystalline, "insoluble" (countercation-free), PB[17,18] also features a rigid cubic framework, except that one-fourth of the $Fe^{II}(CN)_6^{4-}$ units are vacant. It is assumed that water molecules at empty nitrogen positions complete the pseudooctahedral coordination sphere of Fe^{III}. Eight additional H_2O molecules are postulated to exist as isolated molecules in the center of the cell or as water molecules connected by hydrogen bonds to the coordinated ones.[17,18] To explain the existence of complex stoichiometries containing alkali metal countercations (X^+), the formation of solid solutions, e.g., $Fe^{III}_4[Fe^{II}(CN)_6]_3*X_4[Fe^{II}(CN)_6]$, has been postulated.[21]

To address the problems related to the insertion and lattice accommodation of countercations of various sizes, we have chosen cobalt(II) hexacyanoferrate, CoHCNFe, as a model system. Recently, preparation and electrochemical characterization of thin films of CoHCNFe have been reported.[23−29] Among analogues of Prussian Blue, this system has unique properties: its color is dependent not only on the oxidation potential but also on the nature of countercations sorbed from electrolyte during reduction.[26,27] Very recently, it has also been reported that alkali metal cations in the interstitial sites of CoHCNFe can determine the system's electronic and magnetic (spin) states.[16] From a structural viewpoint, the material is attractive

* Corresponding authors.
† University of Warsaw.
‡ Universita di Camerino.
§ Permanent address: Division of General Chemistry, Department of Metallurgy and Materials Engineering, Technical University of Czestochowa, Al. Armii Krajowej 19, PL-42-200 Czestochowa, Poland.

S1089-5647(97)02649-7 CCC: $15.00
Published on Web 02/20/1998

because it is characterized by (1) a perfect, or almost perfect, linear atomic chain, (2) high degeneration of the chain, and (3) short distances between Fe and Co.[30] In the present study, we try to put together the results of electrochemical, microgravimetric, visible spectrophotometric, and X-ray absorption spectroscopic studies. Since the electrochemically grown and reductively cycled metal hexacyanoferrate films are believed to have compositions intermediate between the "soluble" and "insoluble" formulas, we concentrate here on more defined microcrystalline precipitates. Our observations imply that the choice of a alkali metal cation has a profound effect on color, redox behavior, and structure (chemical environment of Co^{II} ions) of reduced CoHCNFe. We believe that some of these conclusions may be generalized for other cyanometalate systems.

Experimental Section

Unless otherwise stated, all chemicals were of analytical grade purity and were used as received. Sodium ferrocyanide decahydrate (assay >97%) was obtained from Fluka (Buchs, Switzerland). The following cobalt(II) hexacyanoferrate(II) samples, $Na_2Co^{II}[Fe^{II}(CN)_6]*nH_2O$, $Li_2Co^{II}[Fe^{II}(CN)_6]*nH_2O$, or $Cs_2Co^{II}[Fe^{II}(CN)_6]*nH_2O$, were prepared by precipitation via dropwise mixing of equivalent amounts of 0.04 mol dm^{-3} solutions: $Na_4[Fe(CN)_6]$ with $CoCl_2$ (each containing NaCl, LiCl, or CsCl, respectively, at 1 mol dm^{-3} level). The resulting precipitates were filtered and rinsed: first, with the respective NaCl, LiCl, or CsCl electrolyte, respectively, and, later, with distilled water. The same procedure was applied to the preparation of $K_2Co^{II}[Fe^{II}(CN)_6]*nH_2O$ ($KCo^{II}[Fe^{III}(CN)_6]*nH_2O$), except that $K_4[Fe(CN)_6]$ ($K_3[Fe(CN)_6]$) and KCl electrolyte were used. $Co^{II}_2[Fe^{II}(CN)_6]*nH_2O$ was precipitated by mixing solutions 0.2 mol dm^{-3} $CoCl_2$ with 0.04 mol dm^{-3} $Na_4[Fe(CN)_6]$ and then rinsed with the $CoCl_2$ solution and, later, with water. All precipitates were air-dried at ambient conditions (temperature, ca. 20 °C; relative humidity, approximately 80%). Under such conditions, the materials were hydrated (interstitial and absorbed water) to the extent 8−11 H_2O, as it was estimated from the hydrogen determinations in elemental analysis.

Electrochemical measurements were done with a CH Instruments (Cordova, TN) model 660 analyzer. Electrodes used for cyclic voltammetry were paraffin-impregnated graphite substrates (geometric area, 0.13 cm^2) which were prepared as described elsewhere.[31] Electrochemical quartz crystal microbalance measurements were performed with the use of gold-coated AT-cut 9 MHz quartz crystals (disks) of geometrical area 0.50 cm^2.[11] The system was characterized by mass sensitivity, 5.89×10^{-9} g cm^{-2} Hz^{-1}. Frequency responses (with resolution of 0.1 Hz) were measured using a Fluke-Phillips (Netherlands) model PM6680B universal counter. A small amount (on a milligram level) of the finely ground CoHCNFe was transferred and distributed uniformly on the surface of a gold-coated electrode by gentle rubbing as described before.[31] Such modified electrode was rinsed with distilled water. The electrochemical experiments were performed in a three-electrode cell using a Pt wire counter and a saturated (KCl) calomel reference electrode.

Visible spectra of dispersed CoHCNFe were recorded using a Hewlett-Packard 8452A diode array spectrophotometer. Solids were first prepared as gels, i.e., from CoHCNFe precipitates that were centrifuged at 3000 rpm. Then, the material was transferred onto the surface of a conventional microscopic glass slide. To produce a uniform layer (thickness, ca. 50 μm), the gels were carefully spreaded (painted) with another glass slide. The CoHCNFe-coated glass slide was dried for 30 min.

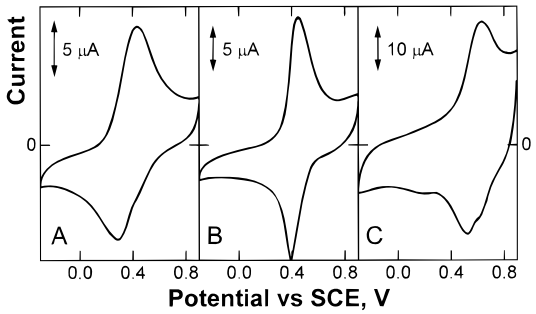

Figure 1. Cyclic voltammograms of CoHCNFe particles mechanically attached to paraffin-impregnated graphite electrodes recorded in 1 mol dm^{-3} (A) LiCl, (B) NaCl, and (C) KCl electrolytes. Scan rate: 50 mV s^{-1}. Following CoHCNFe precipitates, (A) $LiCo^{II}[Fe^{III}(CN)_6]$, (B) $NaCo^{II}[Fe^{III}(CN)_6]$, and (C) $KCo^{II}[Fe^{III}(CN)_6]$ were initially attached to electrode surfaces.

Cobalt hexacyanoferrate films, dispersed on graphite foil (Goodfellow, Cambridge, England), were subjected to energy-dispersive X-ray analysis (EDX) on a Leica-Cambridge 360 scanning electron microscope equipped with an EDX probe. Both EDX and elemental analysis data support the 1:1 stoichiometry of Co to Fe, and they confirm the presence of alkali metal cations in CoHCNFe precipitates: $K_2Co^{II}[Fe^{II}(CN)_6]*nH_2O$, $Na_2Co^{II}[Fe^{II}(CN)_6]$, $Li_2Co^{II}[Fe^{II}(CN)_6]$, $Cs_2Co^{II}[Fe^{II}(CN)_6]$, and $KCo^{II}[Fe^{III}(CN)_6]$.

X-ray absorption spectroscopy (XAS) measurements were carried out at Daresbury Laboratory (England). They were performed in transmission mode on powdered compounds at 8.1 line with a positron beam energy of 2.0 GeV and with a typical current of 300 mA. The XAS measurements were done at Fe K-edge and Co K-edge using the Si(311) double-crystal monochromator. Harmonics signals were rejected by detuning. X-ray absorption near-edge spectra were collected in the ranges 7040−7240 eV (Fe K-edge) and 7640−7840 eV (Co K-edge) at 0.3 eV steps with an integration time of 2 s. Samples were prepared in Millipore pellets. Optimization of samples and preliminary measurements were carried out using an EXAFS Rigaku machine located at CIGA, University of Camerino.

All experiments were performed at room temperature (20−21 °C). High-purity nitrogen was used to deoxygenate the solutions, although the electrochemical behavior was, in general, not sensitive to oxygen in the range of potentials investigated.

Results and Discussion

Electrochemical and Microgravimetric Measurements. Figure 1 compares cyclic voltammetric responses obtained when paraffin-impregnated graphite electrodes containing mechanically attached $Li_2Co^{II}[Fe^{II}(CN)_6]*nH_2O$ (curve A), $Na_2Co^{II}[Fe^{II}(CN)_6]*nH_2O$ (curve B), and $K_2Co^{II}[Fe^{II}(CN)_6]*nH_2O$ (curve C) were placed in the respective 1 mol dm^{-3} electrolytes: (A) LiCl, (B) NaCl, and (C) KCl. The processes, which are observed at formal (midpeak) potentials (A) 0.345, (B) 0.420, and (C) 0.585 V, correspond to the reaction given in eq 1:[20,23,24]

$$XCo^{II}[Fe^{III}(CN)_6] + e^- + X^+ \rightleftarrows X_2Co^{II}[Fe^{II}(CN)_6] \quad (1)$$

where X^+ is Li^+, Na^+, or K^+. Equation 1 implies a direct involvement of a countercation in the redox process.

To verify the insertion of X^+ countercation during reduction and its exclusion upon oxidation, we have measured mass changes at the electrode/solution interface by monitoring changes in resonance frequency of a quartz crystal used as a working electrode. Previously, we employed electrochemical

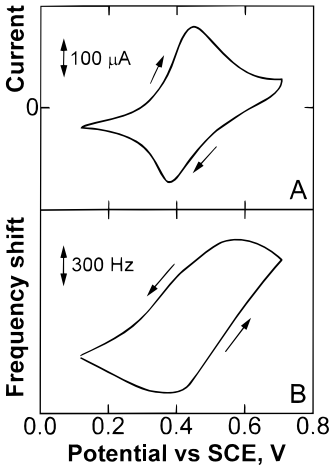

Figure 2. Simultaneous (A) cyclic voltammetric and (B) microgravimetric (EQCM) responses recorded for CoHCNFe particles mechanically attached to gold-coated quartz crystals. Electrolyte: 1 mol dm^{-3} NaCl. Scan rate: 10 mV s^{-1}. CoHCNFe particles were initially in a form of $NaCo^{II}[Fe^{III}(CN)_6]$.

quartz crystal microbalance (EQCM) to study sorption of alkali metal cations and associated water molecules during redox reactions of nickel hexacyanoferrate film.[11] In the present work, we address the transport of ions in solid particles of CoHCNFe that are mechanically attached to gold-coated crystals using the approaches developed earlier.[31,32] Consequently, we investigate the sorption of X^+ into an array of microcrystalline CoHCNFe particles on the electrode surface rather than into the thin electrodeposited film[26,27] which may be structurally different from the respective precipitate. Figure 2 illustrates mass changes of dispersed CoHCNFe during a cyclic voltammogram (curve A) in 1 mol dm^{-3} NaCl at 10 mV s^{-1}. At this scan rate, the system is expected to reach equilibrium conditions.[11] A rise of frequency (mass decrease) was observed in EQCM during the oxidation cycle, and the opposite effect was seen during reduction (curve B). Analogous EQCM patterns have been obtained in the electrolytes containing K^+ or Li^+. A comparison of frequency change, which is equivalent to mass change (5.14 μg cm^{-2}), with the respective charge (15.2 mC cm^{-2}), or number of moles (1.57×10^{-7} mol cm^{-2}), consumed during oxidation (Figure 2) yields the value of 32.6 g mol^{-1}, which implies that ca. 0.5 water molecules are transferred by a Na^+ cation. It comes from the additional EQCM experiments performed in KCl and LiCl (for simplicity not shown here) that, approximately, 0.3 and 1.4 water molecules are transferred by K^+ and Li^+ cations. Although the values obtained are lower than the typical hydration numbers of alkali cations, they are in agreement with the order of hydration abilities of the ions. The data compare well with the results obtained earlier for a film of nickel hexacyanoferrate.[11] In the above estimations, we have assumed, as before,[11] that neutrality is preserved at all times, and anions play no role in the redox mechanism. Further, we have not considered a possibility of expulsion of water molecules upon uptake of a countercation. Regardless of the actual mechanism, the net amount of water molecules transferred (together with countercations) into CoHCNFe upon reduction reflects the degree of hydration of sorbed counterions.

It has been reported[26] that exposure of thin CoHCNFe films to solutions containing CsCl or $CoCl_2$ makes the system almost electroinactive after a few voltammetric potential cycles in the respective supporting electrolytes. We demonstrate here using EQCM that both Cs^+ (Figure 3A) and Co^{2+} (Figure 3B) are capable of exchanging a countercation (K^+ or Na^+) and entering

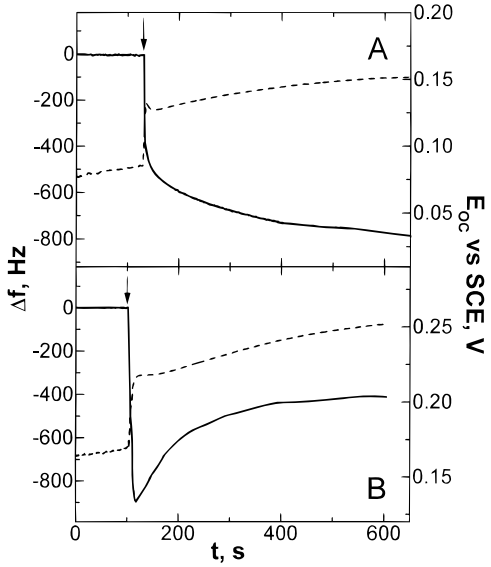

Figure 3. Simultaneous EQCM monitoring of frequency (Δf) changes (solid lines) and open-circuit potential (E_{oc}) changes (dashed lines) following exposure of (A) $Na_2Co^{II}[Fe^{II}(CN)_6]$ and (B) $K_2Co^{II}[Fe^{II}(CN)_6]$, which were mechanically attached to a gold-coated quartz crystal electrode, to (A) 0.1 mol dm^{-3} $CsNO_3$ and (B) 0.2 mol dm^{-3} $Co(NO_3)_2$. Arrows indicate moments at which the respective salts were added to water under stirring conditions.

the phase of microcrystalline solid CoHCNFe particles that have been mechanically attached to gold-coated quartz crystals. Before injections of concentrated Cs^+ (Figure 3A) or Co^{2+} (Figure 3B) solutions, CoHCNFe has been equilibrated in water for ca. 5 min. Following injections (marked with arrows in Figure 3), frequency responses markedly decrease, thus implying incorporation of Cs^+ and Co^{2+}. The process is accompanied by changes of open-circuit potentials (dotted lines in Figure 3). Although the degree of hydration of transferred cations is unknown, molar weights of cesium and cobalt ions are expected to be higher than those of potassium and sodium cations, respectively. Consequently, the uptake of Cs^+ and Co^{2+}, and the related EQCM frequency decreases, can be interpreted in terms of simultaneous replacement of K^+ or Na^+ counterions. EQCM frequency increases, which have been observed at longer exposures of CoHCNFe to Co^{2+} solution (Figure 3B), are presumably due to the material's dissolution or the delayed release of exchanged Na^+ cations. Regardless of the actual mechanism, it comes from the data of Figure 3 that, following insertion of Cs^+ and Co^{2+}, the cations are trapped within the CoHCNFe structure. It is likely that Cs^+ is not capable of retaining a hydration shell,[12,26] or it expels structural water molecules upon entering the system's lattice;[12,33] Co^{2+} ions are likely to be electrostatically attracted in the membrane-like CoHCNFe.

Redox potential shifts induced by the replacements of alkali metal cations in the electrolytes (Figures 1 and 3) were also evident in other metal hexacyanoferrates.[34,35] A linear relationship between potential and ionic radius was reported for nickel hexacyanoferrate[34] and for PB.[35] The order of increase of dehydrated ionic radii (in nanometers) of Li^+ (0.060), Na^+ (0.095), K^+ (0.133), and Cs^+ (0.169) is opposite that of the respective sequence of diameters for hydrated cations (in nanometers): Li^+ (0.42), Na^+ (0.36), K^+ (0.24), and Cs^+ (0.23).[35−37] In the present work, the system's midpeak (formal) potentials obtained in LiCl, NaCl, and KCl (Figure 1) correlate well with the ionic radii (direct proportionality: slope, 3.35 ± 0.60 V nm^{-1}; correlation, $R = 0.9846$) and, even better, with

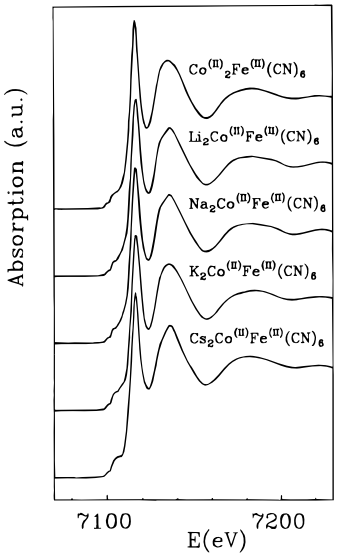

Figure 4. XANES spectra of cobalt(II) hexacyanoferrate(II) containing various alkali metal cations taken at the K-absorption edge of Fe.

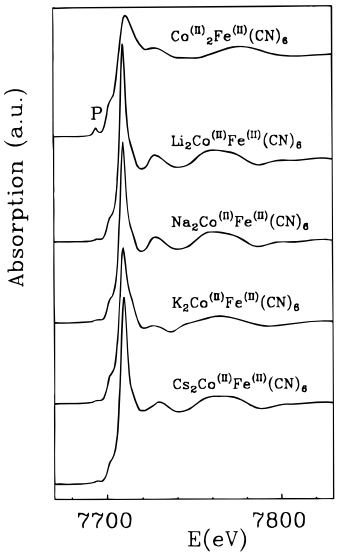

Figure 5. XANES spectra of cobalt(II) hexacyanoferrate(II) containing various alkali metal cations taken at the K-absorption edge of Co.

the hydrated ionic radii (indirect proportionality: slope, -1.35 ± 0.01 V nm^{-1}; correlation, $R = 0.9999$). Since a cavity radius for cobalt hexacyanoferrate is 0.180 nm,[38] it is likely that alkali metal countercations do not retain a complete hydration shell when they enter the system's lattice. The differences in hydration energies (in volts) for Li^+ (5.07), Na^+ (4.08), K^+ (3.34), and Cs^+ (2.45) are significant in aqueous solutions.[35] They are much larger than the differences observed for midpeak (formal) potentials (Figure 1). This observation may be explained, as before for PB,[35] in terms of a partial dehydration of the cations that makes them to be of the appropriate size to enter the crystal's lattice. The process would require enough energy to make the differences in formal potentials smaller. Our EQCM data are also consistent with the partial dehydration of countercations upon entrance to the crystal lattice.

X-ray Absorption Characterization. Figures 4 and 5 show the respective K-edge X-ray absorption near-edge structure (XANES) spectra of iron and cobalt ions in the series of reduced cobalt(II) hexacyanoferrate(II) powders containing various alkali metal cations. For comparison, we provide the spectrum of a "normal" system, $Co^{II}{}_2[Fe^{II}(CN)_6]$, which contains no counter-

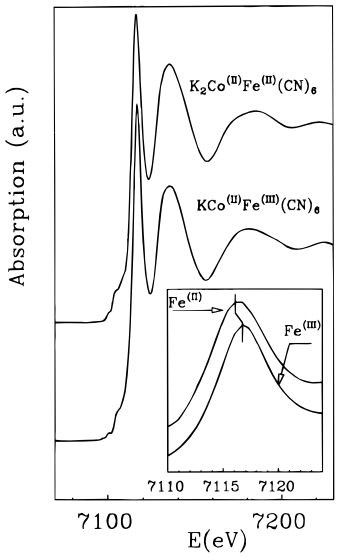

Figure 6. XANES spectra of the oxidized and reduced CoHCNFe recorded at the K-absorption edge of Fe. The inset magnifies the edge region.

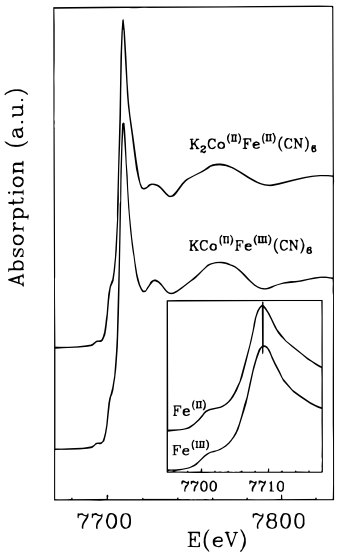

Figure 7. XANES spectra of the oxidized and reduced CoHCNFe recorded at the K-absorption edge of Co. The inset magnifies the edge region.

cation. The Fe K-edge spectra of various cobalt(II) hexacyanoferrate(II) powders are practically identical (Figure 4). Only when the system has been investigated in the oxidized form, as cobalt(II) hexacyanoferrate(III), has the position of the Fe K-edge shifted, and $KCo^{II}[Fe^{III}(CN)_6]$ has an energy ca. 1 eV higher in comparison to $K_2Co^{II}[Fe^{II}(CN)_6]$ (Figure 6). But there are certain differences in the Co K-edge spectra of cobalt(II) hexacyanoferrates(II) (Figure 5). It also comes from the comparison of XANES spectra of $K_2Co^{II}[Fe^{II}(CN)_6]$ and KCo^{II}-$[Fe^{III}(CN)_6]$ in the vicinity of the K-absorption edge of Co (Figure 7) that the oxidation state of cobalt(II) is in both cases the same.

Careful examination of the data of Figure 5 shows that the Co K-edge spectrum of counterion-free $Co^{II}{}_2[Fe^{II}(CN)_6]$ differs from the respective spectra of other systems that contain alkali metal cations. A well-defined peak (P) in the preedge region can be clearly detected in the case of $Co^{II}{}_2[Fe^{II}(CN)_6]$. This peak is assigned to the formally forbidden electronic transition, 1s−3d, that becomes partially allowed in a nonperfect, centrosymmetric, complex.[39] It is likely that incorporation of

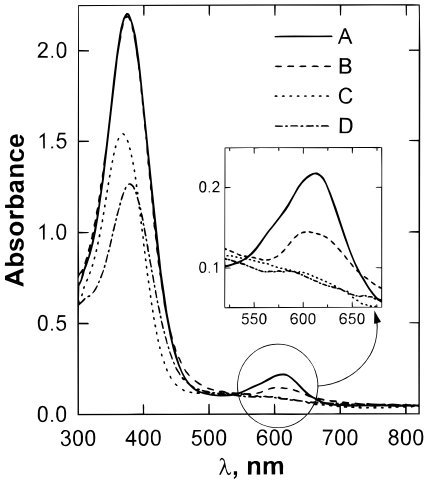

Figure 8. Visible spectra of reduced CoHCNFe precipitates (A) $Li_2Co^{II}[Fe^{II}(CN)_6]*nH_2O$, (B) $Na_2Co^{II}[Fe^{II}(CN)_6]*nH_2O$, (C) $K_2Co^{II}[Fe^{II}(CN)_6]*nH_2O$, and (D) $Cs_2Co^{II}[Fe^{II}(CN)_6]*nH_2O$, which were dispersed and mechanically attached to glass slides.

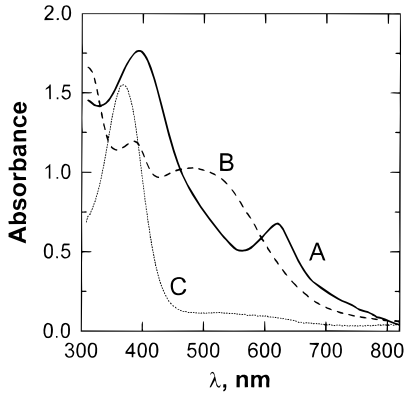

Figure 9. Visible spectra of CoHCNFe precipitates dispersed and mechanically attached to glass slides: (A) $Co^{II}_2[Fe^{II}(CN)_6]*nH_2O$, (B) $KCo^{II}[Fe^{III}(CN)_6]*nH_2O$, and (C) $K_2Co^{II}[Fe^{II}(CN)_6]*nH_2O$.

relatively small cobalt(II) cations into the system's cubic lattice[1,12,21,27] deforms the perfectly octahedral environment of structural cobalt(II). The fact that the peak, which describes first coordination shell distance (around Co), appears in $Co^{II}_2[Fe^{II}(CN)_6]$ at higher energy (7780 eV) than in the other compounds (Figure 5) is consistent with shorter Co−N bond length in "normal" $Co^{II}_2[Fe^{II}(CN)_6]$. It is noteworthy that the latter system shows unique electrochemical and spectrochemical characteristics. The electrodes modified with thin films of this "normal" cobalt hexacyanoferrate are practically electroinactive. Further, we have found from spectrophotometric measurements that these films exhibit a specific, deep green, color (Figure 9, spectrum A).

Upon comparison of high-energy (>7750 eV) peaks in the XANES spectra (Figure 5) of alkali-metal-containing cobalt(II) hexacyanoferrates(II), we have found that the first coordination shell distances (Co−N bond lengths) seem to be shorter in $K_2Co^{II}[Fe^{II}(CN)_6]$ and $Cs_2Co^{II}[Fe^{II}(CN)_6]$ than in $Na_2Co^{II}[Fe^{II}(CN)_6]$ and $Li_2Co^{II}[Fe^{II}(CN)_6]$. Such a statement has been based on the fact that the main EXAFS oscillation appears at higher energy when the bond is shorter.[40] The phenomenon presumably originates from the fact that the hydrated potassium and cesium ions are smaller than hydrated sodium and lithium cations. We assume that alkali metal cations enter the system's lattice in the hydrated form. Even if these ions are partially dehydrated in the system's structure, the actual degrees of hydration and ionic sizes are likely to follow the order typical

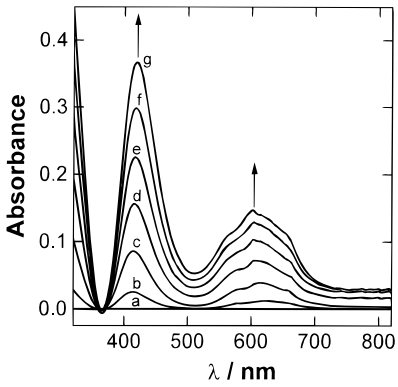

Figure 10. Visible spectra of $K_2Co^{II}[Fe^{II}(CN)_6]*nH_2O$ precipitate (dispersed and mechanically attached to a glass slide) recorded at temperatures (a) 25, (b) 35, (c) 45, (d) 55, (e) 65, (f) 75, and (g) 85 °C. The sample was heated at a rate of 3 °C min^{-1}.

for alkali metal cations in aqueous solutions: $Li^+(aq) > Na^+(aq) > K^+(aq) > Cs^+(aq)$.

Visible Absorption Spectra. Previously, we demonstrated that thin CoHCNFe films were not only electrochromic but their color was also dependent on the nature of alkali metal cations sorbed from a supporting electrolyte during reduction.[26] We present here the results of spectrophotometric measurements that have been done on CoHCNFe precipitates which are virtually the same as for X-ray absorption spectroscopy. They contained various countercations, and they have been dispersed and attached to glass substrates. It is apparent from Figure 8 that the visible spectra of CoHCNFe depend on the choice of an alkali metal countercation. While $Li_2Co^{II}[Fe^{II}(CN)_6]*nH_2O$ is green (Figure 8, spectrum A) and $Na_2Co^{II}[Fe^{II}(CN)_6]*nH_2O$ is olive-green (Figure 8, spectrum B), $K_2Co^{II}[Fe^{II}(CN)_6]*nH_2O$ and $Cs_2Co^{II}[Fe^{II}(CN)_6]*nH_2O$ are light brown (Figure 8, spectra C and D). As we have already mentioned, the color of $Co^{II}_2[Fe^{II}(CN)_6]*nH_2O$ is deep green (Figure 9, spectrum A). Obviously, the color of CoHCNFe depends on the system's oxidation state: a spectrum (Figure 9B) of the oxidized $KCo^{II}[Fe^{III}(CN)_6]*nH_2O$ (which is purple-brown) is markedly different from that of the reduced form (Figure 9C). The latter observation is in agreement with the results of our previous studies concerning electrochromicity of thin films of CoHCNFe.[26,27,42]

To explain distinct colors of CoHCNFe containing various countercations (Figure 8), it is important to appreciate the fact that coloring of cobalt compounds usually reflects the degree of aquation of Co^{II} in the structure. Thermochromism of cobalt salts is also explained in this way.[41] We demonstrate here (Figure 10) that the dispersed layers of $K_2Co^{II}[Fe^{II}(CN)_6]*nH_2O$ are thermochromic, and their color slowly turns from olive-brown to green upon increase of temperature from 25 to 85 °C. The thermochromic effect is reversible, and it presumably reflects changes in the coordination environment of Co^{II}, most likely, in the degree of interaction of water molecules with Co^{II} ions.[41] When a heated green sample (as for Figure 10, curve e) was allowed to cool (to 25 °C, and later down to 0 °C) in the dry atmosphere of a desiccator with P_2O_5, an initial olive-brown color (as for Figure 10, curve a) was not reestablished. Therefore, we think that the chromicity of the material is related to the reversible uptake of water.

Upon comparison of data of Figures 8 and 10, it can be expected that cobalt(II) is less aquated also in green sodium- and lithium-containing films. Our voltammetric and EQCM data are consistent with the view that the degree of hydration of alkali metal cations in the CoHCNFe lattice follow the same order as in solution. Because hydrated Na^+ and Li^+ are larger

than hydrated K^+ and Cs^+ ions, the latter ions are expected to be more easily accommodated at interstices (cavities) in a rigid framework of cobalt(II) hexacyanoferrate(II). Consequently, any contribution from the hydration shell of a countercation to the aquation environment of structural Co^{II} is likely to be higher in the case of potassium and cesium ions. An alternate or supplementary explanation may take into account differences in the attraction forces between the countercations and structural water. If we assume the order for aqueous solutions, the H_2O molecules should be more strongly attracted by Li^+ and Na^+ than K^+ and Cs^+ ions. Another possibility is that different chemical identities of intercalated alkali metal cations may induce variations in the crystal field about the cobalt center. Such variations would be expected to induce a shift in the crystal field parameters: deformations of d−d bands and intervalent charge-transfer transitions. The fact that ligand bond lengths vary as a function of intercalated cation (X-ray data) would be in agreement with such a hypothesis. At present, we do not have any other experimental results supporting the case.

Conclusions

Both voltammetric and EQCM investigations of solid CoHCNFe particles after mechanical transfer onto an electrode surface imply that alkali metal countercations are incorporated into the reduced structures. It is possible that these ions do not retain a complete hydration shell upon entrance to the system's lattice. Nevertheless, the order of their degrees of hydration resembles the sequence observed in aqueous solutions. A linear relationship (with negative slope) has been found between the system's reduction (formal) potentials and the hydrated ionic radii of Li^+, Na^+, and K^+. CoHCNFe is largely electroinactive in Cs^+ and Co^{2+} electrolytes; both ions are trapped at interstitial positions rather than lattice positions. The interstitial crystallographic positions (cavities) are typically occupied by countercations or water molecules.[5,31,43]

It is apparent from XANES measurements that the chemical environment of Co^{II}, particularly Co−N bond lengths, are dependent on the nature and size of alkali metal cations accommodated in cobalt(II) hexacyanoferrate(II) structures. A possible explanation of spectrophotometric results links the cation-dependent coloring to changes in the environment of structural Co^{II} upon incorporation of alkali metal cations of different sizes and degrees of hydration. The present XANES results of alkali-metal-containing CoHCNFe (reduced) as well as our preliminary EXAFS results[30] are consistent with the existence of rigid, cubic-type, zeolitic structure composed of three orthogonal Fe−C≡N−Co chains in which both metals (Fe and Co) are octahedrally coordinated by six carbons and six nitrogens. Hence, a possibility of direct hydration of lattice Co^{II} ions, e.g., with two H_2O molecules in addition to four −CN− groups as was postulated before,[44] seems to be unlikely. Also, the existence of significant lattice defects, in which a large number of $[Fe(CN)_6]$ sites are vacant, or two chemically distinct Co^{II} sites, as in "normal" $Co^{II}_2[Fe^{II}(CN)_6]$, is improbable. On the other hand, the system's thermochromic behavior clearly implies at least some, perhaps indirect, interactions of structural water molecules with Co^{II}. They may affect Co−N bond lengths or angles. Oxygen atoms from structural water molecules, which are incorporated together with a countercation, are likely to interact with nitrogen atoms from −NC− groups. It has been suggested that spectral changes accompanying solid-state thermochromic effects could involve not only characteristic shifts and deformations of d−d bands, caused by changes in the degree of hydration, strength, and symmetry of the ligand field, but also alterations of charge-transfer bands due to changes in metal−ligand interactions.[41] Further research, including precise EXAFS characterization of all alkali-metal-containing CoHCNFe samples, is in progress along this line.

No differences were found in the Fe K-edge spectra of all investigated cobalt(II) hexacyanoferrate(II) samples recorded at ambient temperature. Only oxidation causes a small shift in the position of the Fe K-edge peak. From a structural point of view, the main difference between the oxidized and reduced systems is the presence of an extra potassium ion in the reduced form. Our preliminary studies[45] show that the extra potassium ion influences the angle Co−N−C that becomes different from 180°. It is not surprising that the color of the oxidized cobalt(II) hexacyanoferrate(III) (deep purple) markedly differs from the colors of reduced samples. In view of a very recent pioneering communication[16] showing a countercation-dependent switching of electronic and spin states in CoHCNFe films at 40 °C, we are currently performing X-ray absorption, electrochemical, and microgravimetric measurements of CoHCNFe at higher temperatures.

Acknowledgment. This work was supported by State Committee for Scientific Research (KBN), Poland, under Grant 3 T09A 120 12 and by the CNR (Rome, Italy). P.J.K. and M.A.M. appreciate travel grants from the University of Camerino.

References and Notes

(1) Sharpe, A. G. *The Chemistry of Cyano Complexes of the Transition Metals*; Academic Press: New York, 1976.
(2) *Mixed-Valence Compounds; Theory and Application in Chemistry, Physics, Geology and Biology*; Brown, D. B., Ed.; Reidel: Dordrecht, 1980; NATO Advanced Study Institute Series C, Vol. 58.
(3) Itaya, K.; Uchida, I.; Neff, V. D. *Acc. Chem. Res.* **1986**, *19*, 162.
(4) Amos, L. J.; Duggal, A.; Mirsky, E. J.; Ragonesi, P.; Bocarsly, A. B.; Fitzgerald-Bocarsly, P. A. *Anal. Chem.* **1988**, *60*, 245.
(5) Kahrlet, H.; Lovrich-Komorowsky, S.; Hermes, M.; Scholz, F. *Fresenius Z. Anal. Chem.* **1996**, *356*, 204.
(6) Monk, P. M. S.; Mortimer, R. J.; Rosseinsky, D. R. *Electrochromism, Fundamentals and Applications*; VCH: Weinheim, 1995; Chapter 6.
(7) Carpenter, M. K.; Connel, R. S.; Simko, S. J. *Inorg. Chem.* **1990**, *29*, 845.
(8) Kulesza, P. J. *Inorg. Chem.* **1990**, *29*, 2395.
(9) Xidis, A.; Neff, V. D. *J. Electrochem. Soc.* **1991**, *138*, 3637.
(10) Feldman, B. J.; Melroy, O. R. *J. Electroanal. Chem.* **1987**, *234*, 213.
(11) Bacskai, J.; Martinusz, K.; Czirok, E.; Inzelt, G.; Kulesza, P. J.; Malik, M. A. *J. Electroanal. Chem.* **1995**, *385*, 241.
(12) Ceranic, T.; Trifunovic, D.; Adamovic, R. *Z. Naturforsch.* **1978**, *33B*, 1099.
(13) Neff, V. D. *J. Electrochem. Soc.* **1985**, *132*, 1382.
(14) Kahn, O. *Nature* **1995**, *378*, 667.
(15) Ferlay, S.; Mallah, T.; Ouahes, R.; Veillet, P.; Verdaguer, M. *Nature* **1995**, *378*, 701.
(16) Sato, O.; Einaga, Y.; Iyoda, T.; Fujishima, A.; Hashimoto, K. *J. Phys. Chem. B* **1997**, *101*, 3903.
(17) Buser, H. J.; Schwarzenbach, D.; Peter, W.; Ludi, A. *Inorg. Chem.* **1977**, *16*, 2704.
(18) Herren, F.; Fischer, P.; Ludi, A.; Halb, W. *Inorg. Chem.* **1980**, *19*, 956.
(19) Keggin, J. F.; Miles, F. D. *Nature* **1936**, *137*, 577.
(20) Hamnett, A.; Higgins, S.; Mortimer, R. J.; Rosseinsky, D. R. *J. Electroanal. Chem.* **1988**, *255*, 315.
(21) Tananaev, I. V.; Seifer, G. B.; Kharitonov, Yu. Ya.; Kuznetsov, V. G.; Korolkov, A. P. *Ferrocyanide Chemistry* (in Russian); Nauka: Moscow, 1971.
(22) Buttry, D. A. In *Electroanalytical Chemistry*; Bard, A. J., Ed.; Dekker: New York, 1992; Vol. 17.
(23) Joseph, J.; Gomathi, H.; Prabhakara Rao, G. *J. Electroanal. Chem.* **1991**, *304*, 263.
(24) Zaldivar, G. A. P.; Gushikem, Y.; Benvenutti, E. V.; de Castro, S. C.; Vasquez, A. *Electrochim. Acta* **1994**, *39*, 33.
(25) Gao, Z.; Bobacka, J.; Ivaska, A. *Electrochim. Acta* **1993**, *38*, 379.

(26) Kulesza, P. J.; Malik, M. A.; Zamponi, S.; Berrettoni, M.; Marassi, R. *J. Electroanal. Chem.* **1995**, *397*, 287.

(27) Kulesza, P. J.; Malik, M. A.; Miecznikowski, K.; Wolkiewicz, A.; Zamponi, S.; Berrettoni, M.; Marassi, R. *J. Electrochem. Soc.* **1996**, *143*, L10.

(28) Cai, C.-X.; Ju, H.-X.; Chen, H.-Y. *J. Electroanal. Chem.* **1995**, *397*, 185.

(29) Chen, S.-M. *J. Electroanal. Chem.* **1996**, *417*, 145.

(30) Giorgetti, M.; Berrettoni, M.; Filipponi, A.; Kulesza, P. J.; Marassi, R. *Chem. Phys. Lett.* **1997**, *275*, 108.

(31) Dostal, A.; Meyer, B.; Scholtz, F.; Schroder, U.; Bond, A. M.; Marken, F.; Shaw, S. J. *J. Phys. Chem.* **1995**, *99*, 2096.

(32) Evans, C. D.; Chambers, J. Q. *Chem. Mater.* **1994**, *6*, 454.

(33) Loss-Neskovic C.; Fedoroff, M. *Solvent Extr. Ion Exch.* **1989**, *7*, 131.

(34) Sinha, S.; Humphrey, B. D.; Bocarsly, A. B. *Inorg. Chem.* **1984**, *23*, 203.

(35) Lundgren, C. A.; Murray, R. W. *Inorg. Chem.* **1988**, *27*, 933.

(36) Robinson, R. A.; Stokes, R. H. *Electrolyte Solutions*, 2nd ed.; Butterworth: London, 1959; pp 120−126.

(37) Cotton, F. A.; Wilkinson, G. *Advanced Inorganic Chemistry*, 4th ed.; Wiley: New York, 1980; pp 762−763.

(38) Jiang, M.; Zhou, X.; Zhao, Z. *Ber. Bunsen-Ges. Phys. Chem.* **1991**, *95*, 720.

(39) Sano, M. *Inorg. Chem.* **1988**, *27*, 4249.

(40) Fay, M. J.; Proctor, A.; Hoffmann, D. P.; Hercules, D. M. *Anal. Chem.* **1988**, *60*, 1225A.

(41) Sone, K.; Fukuda, Y. *Inorganic Thermochromism*; Inorganic Chemistry Concepts 10; Springer-Verlag: Berlin, 1987.

(42) Kulesza, P. J.; Zamponi, S.; Malik, M. A.; Berrettoni, M.; Wolkiewicz, A.; Marassi, R. *Electrochim. Acta*, in press.

(43) Dostal, A.; Kauschka, G.; Reddy, S. J.; Scholz, F. *J. Electroanal. Chem.* **1996**, *406*, 155.

(44) Dubrovin, V. S.; Bryzglova, R. V.; Rogozin, Yu. M. *Russ. J. Inorg. Chem.* **1981**, *26*, 1320.

(45) Berrettoni, M.; Giorgetti, M.; Marassi, R.; Zamponi, S.; Kulesza, P. J. Presented at Euroanalysis IX, Bologna, Abstract No. MoP12, Italy, 1996.